Summarizing multiple aspects of model performance in a single diagram

Karl E. Taylor

Program for Climate Model Diagnosis and Intercomparison, Lawrence Livermore National Laboratory
Livermore, California

Abstract. A diagram has been devised that can provide a concise statistical summary of how well patterns match each other in terms of their correlation, their root-mean-square difference, and the ratio of their variances. Although the form of this diagram is general, it is especially useful in evaluating complex models, such as those used to study geophysical phenomena. Examples are given showing that the diagram can be used to summarize the relative merits of a collection of different models or to track changes in performance of a model as it is modified. Methods are suggested for indicating on these diagrams the statistical significance of apparent differences and the degree to which observational uncertainty and unforced internal variability limit the expected agreement between model-simulated and observed behaviors. The geometric relationship between the statistics plotted on the diagram also provides some guidance for devising skill scores that appropriately weight among the various measures of pattern correspondence.

1. Introduction

The usual initial step in validating models of natural phenomena is to determine whether their behavior resembles the observed. Typically, plots showing that some pattern of observed variation is reasonably well reproduced by the model are presented as evidence of its fidelity. For models with a multitude of variables and multiple dimensions (e.g., coupled atmosphere/ocean climate models), visual comparison of the simulated and observed fields becomes impractical, even if only a small fraction of the model output is considered. It is then necessary either to focus on some limited aspect of the physical system being described (e.g., a single field, such as surface air temperature, or a reduced domain, such as the zonally averaged annual mean distribution) or to use statistical summaries to quantify the overall correspondence between the modeled and observed behavior.

In this paper a new diagram is described that can concisely summarize the degree of correspondence between simulated and observed fields. On this diagram the correlation coefficient and the root-mean-square (RMS) difference between the two fields, along with the ratio of the standard deviations of the two patterns, are all indicated by a single point on a two-dimensional (2-D) plot. Together, these statistics provide a quick summary of the degree of pattern correspondence, allowing one to gauge how accurately a model simulates the natural system. The diagram is particularly useful in assessing the relative merits of competing models and in monitoring overall performance as a model evolves.

The primary aim of this paper is to describe this new type of diagram (section 2) and to illustrate its use in evaluating and monitoring climate model performance (section 3). Methods for indicating statistical significance of apparent differences, observational uncertainty, and fundamental limits to agree-

ment resulting from unforced internal variability are suggested in section 4. In section 5 the basis for defining appropriate "skill scores" is discussed. Finally, section 6 provides a summary and brief discussion of other potential applications of the diagram introduced here.

2. Theoretical Basis for the Diagram

The statistic most often used to quantify pattern similarity is the correlation coefficient. The term "pattern" is used here in its generic sense, not restricted to spatial dimensions. Consider two variables, f_n and r_n, which are defined at N discrete points (in time and/or space). The correlation coefficient R between f and r is defined as

$$R = \frac{\frac{1}{N}\sum_{n=1}^{N}(f_n - \bar{f})(r_n - \bar{r})}{\sigma_f \sigma_r}, \qquad (1)$$

where $\bar{f}$ and $\bar{r}$ are the mean values and σ_f and σ_r are the standard deviations of f and r, respectively. For grid cells of unequal area (1) would normally be modified in order to weight the summed elements by grid cell area (and the same weighting factors would be used in calculating σ_f and σ_r). Similarly, weighting factors for pressure thickness and time interval can be applied when appropriate.

The correlation coefficient reaches a maximum value of 1 when for all n, $(f_n - \bar{f}) = \alpha(r_n - \bar{r})$, where α is a positive constant. In this case the two fields have the same centered pattern of variation but are not identical unless $\alpha = 1$. Thus, from the correlation coefficient alone it is not possible to determine whether two patterns have the same amplitude of variation (as determined, for example, by their variances).

The statistic most often used to quantify differences in two fields is the RMS difference E, which for fields f and r is defined by

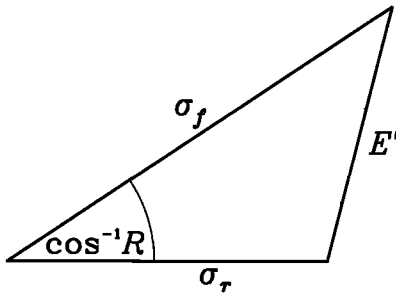$$E = \left[\frac{1}{N}\sum_{n=1}^{N}(f_n - r_n)^2\right]^{1/2}.$$

Figure 1. Geometric relationship between the correlation coefficient R, the centered pattern RMS error E', and the standard deviations σ_f and σ_r of the test and reference fields, respectively.

Again, the formula can be generalized for cases when grid cells should be weighted unequally.

In order to isolate the differences in the patterns from the differences in the means of the two fields, E can be resolved into two components. The overall "bias" is defined as

$$\bar{E} = \bar{f} - \bar{r},$$

and the centered pattern RMS difference is defined by

$$E' = \left\{ \frac{1}{N} \sum_{n=1}^{N} [(f_n - \bar{f}) - (r_n - \bar{r})]^2 \right\}^{1/2}. \qquad (2)$$

The two components add quadratically to yield the full mean square difference:

$$E^2 = \bar{E}^2 + E'^2. \qquad (3)$$

The pattern RMS difference approaches zero as two patterns become more alike, but for a given value of E' it is impossible to determine how much of the error is due to a difference in structure and phase and how much is simply due to a difference in the amplitude of the variations.

The correlation coefficient and the RMS difference provide complementary statistical information quantifying the correspondence between two patterns, but for a more complete characterization of the fields the variances (or standard deviations) of the fields must also be given. All four of the above statistics (R, E', σ_f, and σ_r) are useful in comparisons of patterns, and it is possible to display all of them on a single, easily interpreted diagram. The key to constructing such a diagram is to recognize the relationship between the four statistical quantities of interest here,

$$E'^2 = \sigma_f^2 + \sigma_r^2 - 2\sigma_f\sigma_r R,$$

and the law of cosines,

$$c^2 = a^2 + b^2 - 2ab \cos \phi,$$

where a, b, and c are the lengths of the sides of a triangle and ϕ is the angle opposite side c. The geometric relationship between R, E', σ_f, and σ_r is shown in Figure 1.

With the above definitions and relationships it is now possible to construct a diagram that statistically quantifies the degree of similarity between two fields. One field will be called the "reference" field, usually representing some observed state. The other field will be referred to as a "test" field (typically a model-simulated field). The aim is to quantify how closely the test field resembles the reference field. In Figure 2, two points are plotted on a polar style graph, with the circle representing the reference field and the cross representing the test field. The radial distances from the origin to the points are proportional to the pattern standard deviations, and the azimuthal positions give the correlation coefficient between the two fields. The radial lines are labeled by the cosine of the angle made with the abscissa, consistent with Figure 1. The dashed lines measure the distance from the reference point and, as a consequence of the relationship shown in Figure 1, indicate the RMS error (once any overall bias has been removed).

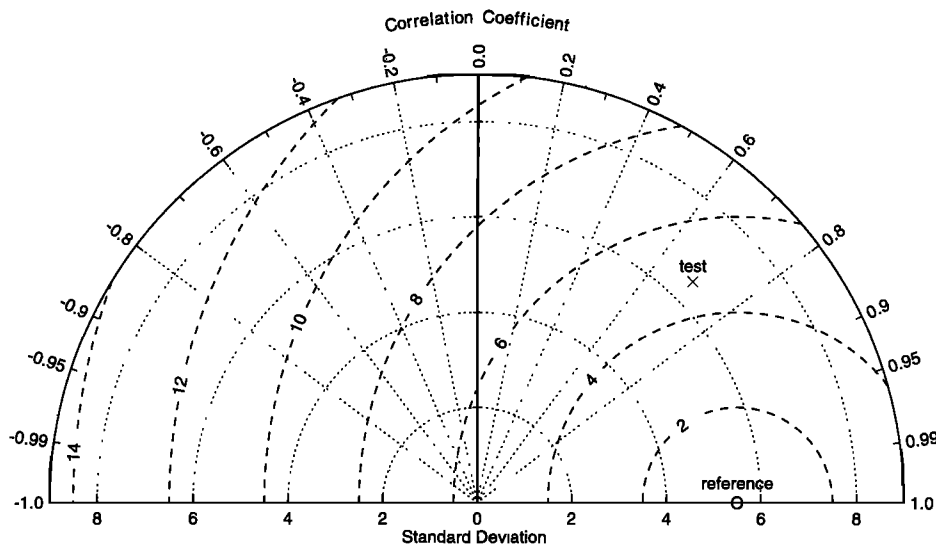The point representing the reference field is plotted along

Figure 2. Diagram for displaying pattern statistics. The radial distance from the origin is proportional to the standard deviation of a pattern. The centered RMS difference between the test and reference field is proportional to their distance apart (in the same units as the standard deviation). The correlation between the two fields is given by the azimuthal position of the test field.

the abscissa. In this example, the reference field has a standard deviation of 5.5 units. The test field lies further from the origin in this example and has a standard deviation of ~6.5 units. The correlation coefficient between the test field and the reference field is 0.7, and the centered pattern RMS difference between the two fields is a little less than 5 units.

3. Two Applications

Construction of an unfamiliar diagram is hardly warranted if, as in the simple example above, only a single pattern is compared to another. In that case one could simply report the values of σ_f, σ_r, R, and E', and a graph would be quite unnecessary. If, however, one wanted to compare several pairs of patterns, as in the following examples, then a diagram can convey the information much more clearly than a table.

3.1. Model Data Comparisons

Plate 1 shows the annual cycle of rainfall over India as simulated by 28 atmospheric general circulation models (GCMs), along with an observational estimate (solid black line). The data are plotted after removing the annual mean precipitation, and both the model and observational values represent climatological monthly means computed from several years of data. The observational estimate shown is from *Parthasarathy et al.* [1994], and the model results are from the Atmospheric Model Intercomparison Project (AMIP), which is described by *Gates et al.* [1999]. Each model is assigned a letter which may be referred to in the following discussion.

Plate 1 shows that models generally simulate the stronger precipitation during the monsoon season but with a wide range of estimates of the amplitude of the seasonal cycle. The precise phasing of the maximum precipitation also varies from one model to the next. It is quite difficult, however, to obtain information about any particular model from Plate 1; there are simply too many curves plotted to distinguish one from another. It is useful therefore to summarize statistically how well each simulated "pattern" (i.e., the annual cycle of rainfall) compares with the observed. This is done in Figure 3 where a letter identifies the statistics computed from each model's results. Figure 3 clearly indicates which models exaggerate the amplitude of the annual cycle (e.g., models K, Q, and C) and which models grossly underestimate it (e.g., models I, V, and P). It also shows which model-simulated annual cycles are correctly phased (i.e., are well correlated with the observed) and which are not. In contrast to Plate 1, Figure 3 makes it easy to identify models that perform relatively well (e.g., models A, O, Z, and N) because they lie relatively close to the reference point. Among the poorer performers it is easy to distinguish between errors due to poor simulation of the amplitude of the annual cycle and errors due to incorrect phasing, as described next. An assessment of whether the apparent differences suggested by Plate 1 and Figure 3 between the models and observations and between individual models are in fact statistically significant will be postponed until section 4.

According to Figure 3 the RMS error in the annual cycle of rainfall over India is smallest for model A. Figure 4 confirms the close correspondence between model A and the observed field. Other inferences drawn from Figure 3 can also be confirmed by Figure 4. For example, models A, B, and C are similarly well correlated with observations (i.e., the phasing of the annual cycle is correct), but the amplitude of the seasonal cycle is much too small in model B and far too large in model

C. Model D, on the other hand, simulates the amplitude reasonably well, but the monsoon comes too early in the year, yielding a rather poor correlation. Thus Figure 3 provides much of the same information as Plate 1 but displays it in a way that allows one to flag problems in individual models.

3.2. Tracking Changes in Model Performance

In another application these diagrams can summarize changes in the performance of an individual model. Consider, for example, a climate model in which changes in parameterization schemes have been made. In general, such revisions will affect all the fields simulated by the model, and improvement in one aspect of a simulation might be offset by deterioration in some other respect. Thus it can be useful to summarize on a single diagram how well the model simulates a variety of fields (among them, for example, winds, temperatures, precipitation, and cloud distribution).

Because the units of measure are different for different fields, their statistics must be nondimensionalized before appearing on the same graph. One way to do this is to normalize for each variable the RMS difference and the two standard deviations by the standard deviation of the corresponding observed field ($\hat{E}' = E'/\sigma_r$, $\hat{\sigma}_f = \sigma_f/\sigma_r$, and $\hat{\sigma}_r = 1$). This leaves the correlation coefficient unchanged and yields a normalized diagram like that shown in Figure 5. Note that the standard deviation of the reference (i.e., observed) field is normalized by itself and it will therefore always be plotted at unit distance from the origin along the abscissa.

In Figure 5 a comparison between two versions of a model is made. The model has been run through a 10-year AMIP experiment with climatological monthly means computed for the 10 fields shown. For each field, two points connected by an arrow are plotted, the tail of the arrow indicating the statistics for the original model version and the head of the arrow indicating the statistics for the revised model. For each of the fields the statistics quantify the correspondence between the simulated and observed time-varying global pattern of each field (i.e., the sums in (1) and (2) run over the 12-month climatology as well as over all longitude and latitude grid cells, weighted by grid cell area). All fields are mapped to a common 4° latitude by 5° longitude grid before computing statistics.

Many of the arrows in Figure 5 point in the general direction of the observed or reference point, indicating that the RMS difference between the simulated and observed fields has been reduced in the revised model. For sea level pressure, the arrow is oriented such that the simulated and observed variances are more nearly equal in the revised model, but the correlation between the two is slightly reduced. For this variable the RMS error is slightly reduced (the head of the arrow lies closer to the observed point than the tail) because the amplitude of the simulated variations in sea level pressure is closer to the observed, even though the correlation is poorer. The overall impression given by Figure 5 is that the model revisions have led to a general improvement in model performance. In order to prove that the apparent changes suggested by Figure 5 are, in fact, statistically significant, further analysis would be required, as discussed in section 4.

4. Indicating Statistical Significance, Observational Uncertainty, and Fundamental Limits to Expected Agreement

In the examples shown in section 3 all statistics have been plotted as points, as if their positions were precise indicators of
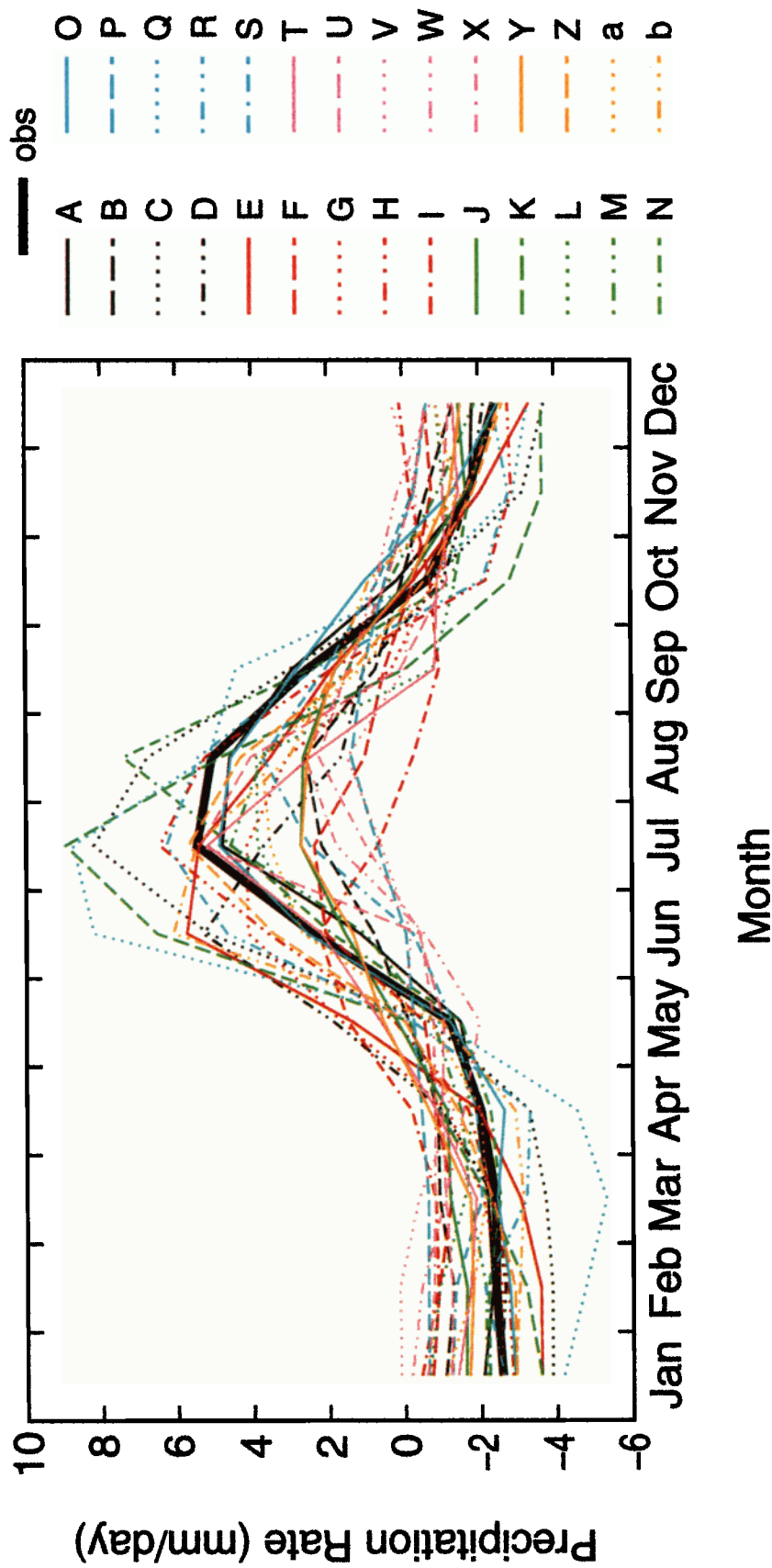
Plate 1. Climatological annual cycle of precipitation over India (with annual mean removed) as observed by *Parthasarathy et al.* [1994] and as simulated by 28 models.
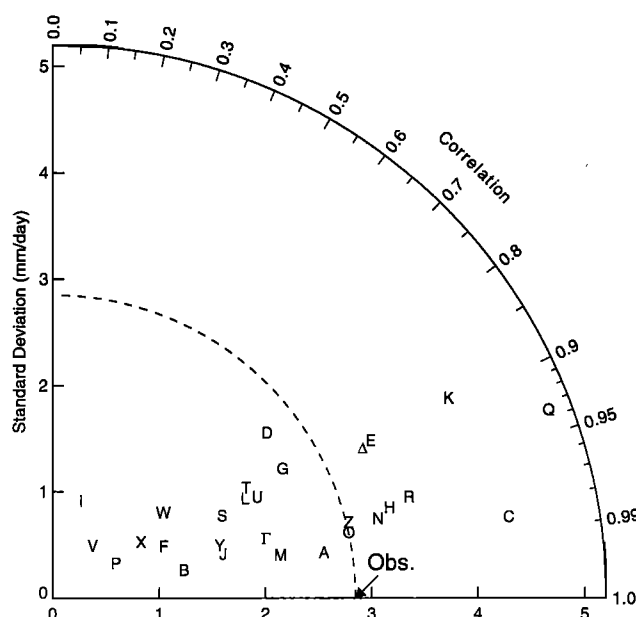
Figure 3. Pattern statistics describing the climatological annual cycle of precipitation over India simulated by 28 models compared with the observed [*Parthasarathy et al.*, 1994]. To simplify the plot, the isolines indicating correlation, standard deviation, and RMS error have been omitted.

the true climate statistics. In practice, the statistics are based on finite samples, and therefore they represent only estimates of the true values. Since the estimates are, in fact, subject to sampling variability, then the differences in model performances suggested by a figure might be statistically insignificant. Similarly, a model that exhibits some apparent improvement in skill may, in fact, prove to be statistically indistinguishable from its predecessor. For proper assessment of model performance the statistical significance of apparent differences should be evaluated.

Another shortcoming of the diagrams, as presented in section 3, is that neither the uncertainty in the observations nor the internal variability, which limits agreement between simulated and observed fields, has been indicated. Even if a perfect climate model could be devised (i.e., a model realistic in all respects), it should not agree exactly with observations that are
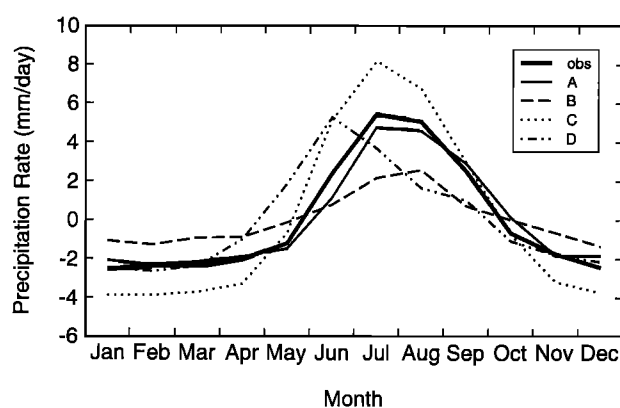

Figure 4. Climatological annual cycle of precipitation over India (with annual mean removed) as observed and as simulated by four models (a subset selected from Plate 1).
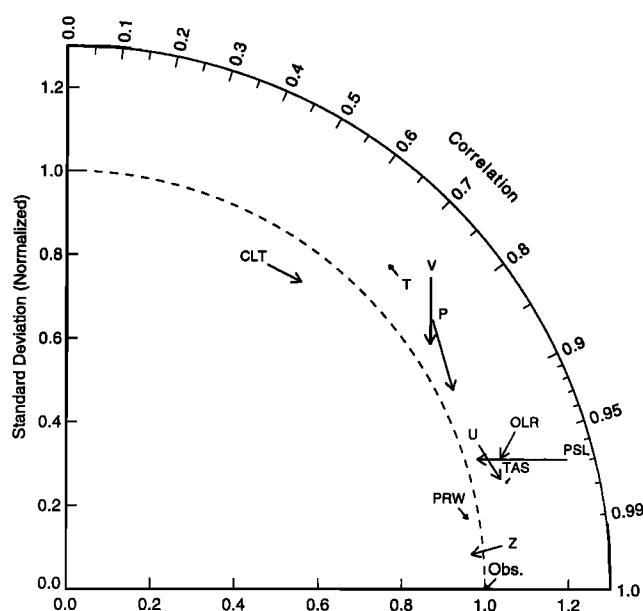
Figure 5. Changes in normalized pattern statistics between two versions of a model. The statistics for the older version of the model are plotted at the tail of the arrows, and the arrows point to the statistics for the revised model. The RMS error and standard deviations have been normalized by the observed standard deviation of each field before plotting. The fields shown are sea level pressure (PSL), surface air temperature (TAS), total cloud fraction (CLT), precipitable water (PRW), 500 hPa geopotential height (Z), precipitation (P), outgoing longwave radiation (OLR), 200 hPa temperature (T), 200 hPa meridional wind (V), and 200 hPa zonal wind (U). The model output and reference (observationally based) data were mapped to a common 4° × 5° grid before computing the statistics. The following reference data sets were used: for OLR, *Harrison et al.* [1990]; for P, *Xie and Arkin* [1997]; for TAS, *Jones et al.* [1999]; for CLT, *Rossow and Schiffer* [1991]; and for all other variables, *Gibson et al.* [1997].

to some extent uncertain and inaccurate. Moreover, because a certain fraction of the year-to-year differences in climate are not deterministically forced but arise due to internal instabilities in the system (e.g., weather "noise", quasi-biennial oscillation, El Niño–Southern Oscillation, etc.), the climate simulated by a model, no matter how skillful, can never be expected to agree precisely with observations, no matter how accurate.

In the verification of weather forecasts this latter constraint on agreement is associated primarily with theoretically understood limits of predictability. In the evaluation of coupled atmosphere/ocean climate model simulations started from arbitrary initial conditions the internal variability of the model should be expected to be uncorrelated with the internal component of the observed variations. Similarly, in atmospheric models forced by observed sea surface temperatures, as in AMIP, an unforced component of variability (in part due to weather noise) will limit the expected agreement between the simulated and observed fields.

4.1. Statistical Significance of Differences

One way to assess whether or not the apparent differences in model performance shown in Figure 3 are, in fact, significant is to consider an ensemble of simulations obtained from one or more of the models. For AMIP-like experiments such an en-
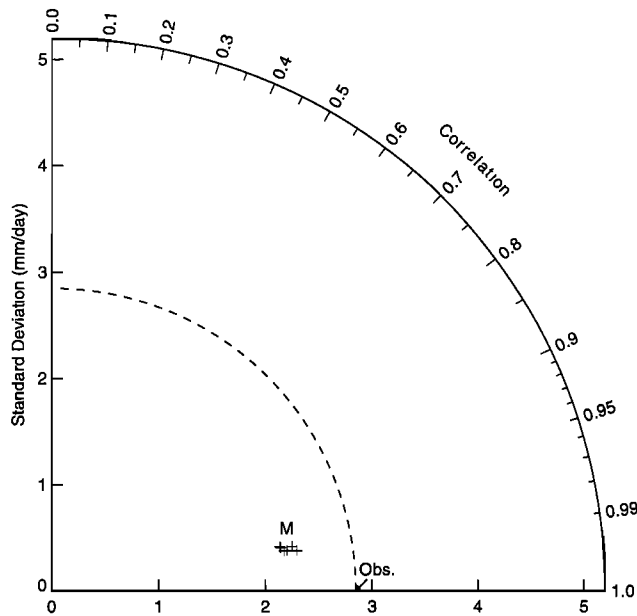
Figure 6. Pattern statistics describing the modeled and observed climatological annual cycle of precipitation over India computed from six independent simulations by model M. The close clustering of pluses calculated from the model M ensemble indicates that the differences between models shown in Figure 3 are generally likely to be statistically significant.

semble is typically created by starting the simulations from different initial conditions but forcing them with the same time-varying sea surface temperatures and sea ice cover. Thus the weather (and to a much lesser extent the climate statistics) will differ between each pair of realizations.

In the case of rainfall over India, results were obtained from a six-member ensemble of simulations by model M. The statistics comparing each independent ensemble member to the observed are plotted as individual symbols below the M in Figure 6. The close grouping of pluses in the diagram indicates that the uncertainty in the point location attributable to sampling variability is not very large. A formal test for statistical significance could be performed based on the spread of points in Figure 6, but for a qualitative assessment this is unnecessary. If model M is typical, then the relatively large differences between model climate statistics seen in Plate 1 are likely to indicate true differences in most cases. The differences are unlikely to be explained simply by the different climate "samples" generated by simulations of this kind. A similar approach for informally assessing statistical significance could be followed to determine whether the model improvements shown in Figure 5 are statistically significant.

One limitation of this approach to assessing statistical significance is that it accounts only for the sampling variability in the model output, not in the observations. Although an estimate of the impact of sampling variability in the observations will not be carried out here, there are several possible ways one might proceed. One could split the record into two or more time periods and then analyze each period independently. The differences in statistics between the subsamples could then be attributed to both real differences in correspondence between the simulated and observed fields and differences due to sampling variability. With this approach an upper limit on the sampling variability could be established. Another approach

would be to use an ensemble of simulations by a single model as an artificial replacement for the observations. A second ensemble of simulations by a different model could then be compared to a single member of the first ensemble, generating a plot similar to Figure 6. The effects of sampling variability in the observations could then be assessed by comparing the second ensemble to the other members of the first ensemble and quantifying the increase in the spread of points. If the sampling distribution of the first ensemble were similar to the sampling distribution of the observed climate system, then the effects of sampling variability could be accurately appraised. A third option for evaluating the sampling variability, at least in the comparison of climatological data computed from many time samples, would be to apply "bootstrap" techniques to sample both the model output and the observational data. If such a technique were used, care would be required to account for the temporal and spatial correlation structure of the data [*Wilks*, 1997].

4.2. Observational Uncertainty

Because of a host of problems in accurately measuring regional precipitation, observational estimates are thought to be highly uncertain. When two independent observational estimates can be obtained that are thought to be of more or less comparable reliability, then the difference between the two can be used as an indication of observational uncertainty. As an illustration of this point, an alternative to the India rainfall estimate is plotted in Figure 7 based on data from *Xie and Arkin* [1997]. Also plotted for comparison are model results, which will be discussed later in this section. The distance between the point labeled Xie-Arkin and the reference point
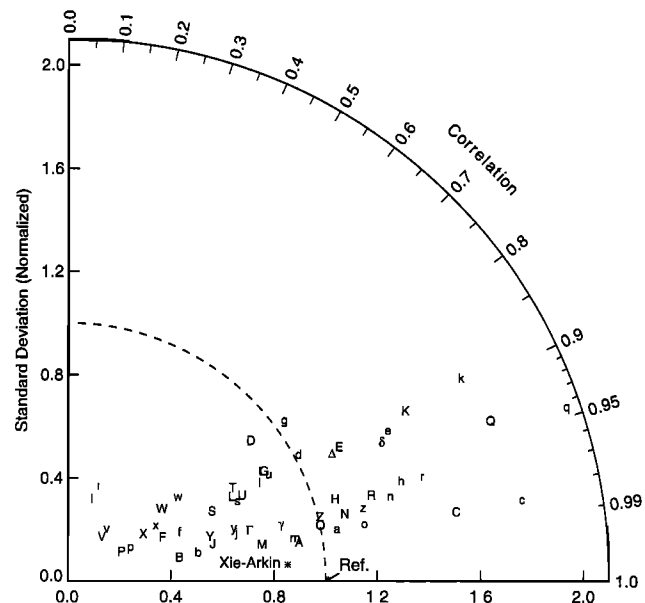

Figure 7. Normalized pattern statistics showing differences between two observational estimates of rainfall (the reference data set given by *Parthasarathy et al.* [1994] and the alternative data set (indicated by an asterisk) given by *Xie and Arkin* [1997]). Also shown are differences between the 28 models and each of the reference data sets (uppercase letters for the 28 models compared to the *Parthasarathy et al.* [1994] reference and lowercase letters for the 28 models compared to the *Xie and Arkin* [1997] reference).

(referring to observations from *Parthasarathy et al.* [1994]) provides one measure of observational uncertainty, although one should be aware that the two data sets are not truly independent. The correlation between the two observational estimates is very high (0.997), but the amplitude of the seasonal cycle is substantially smaller according to the *Xie and Arkin* [1997] data. If both observational estimates were equally believable, then one should not expect the RMS differences between the models and the reference observational data set to be smaller than the differences between the two observational data sets.

The other points plotted in Figure 7, labeled with letters, indicate model results. The capital letters reproduce the results of Figure 3 in which the models were compared to the *Parthasarathy et al.* [1994] observational data. The corresponding lowercase letters indicate the statistics calculated when the same model results are compared with the *Xie and Arkin* [1997] observational data. Thus the reference for the capital letters (and for the point labeled Xie-Arkin) is the *Parthasarathy et al.* [1994] data, and the reference for the lowercase letters is the *Xie and Arkin* [1997] data. Note that for all models the normalized standard deviation increases by the ratio of the variances of the two observational data sets, but for most models the correlation with each of the observational data sets is similar. In a few cases, however, the correlation can change; compare, for example, differences between G and g and D and d.

Another way to compare model-simulated patterns to two different reference fields is to extend the diagram to three dimensions. In this case one of the reference points (obs1) would be plotted along one axis (say the *x* axis) and the other (obs2) would be plotted in the *xy* plane indicating its statistical relationship to the first. One or more test points could then be plotted in 3-D space such that the distance between each test point and each of the reference points would be equal to their respective RMS differences. Distances from the origin would again indicate the standard deviation of each pattern, and the cosines of the three angles defined by the position vectors of the three points would indicate the correlation between the pattern pairs (i.e., model-obs1, model-obs2, and obs1-obs2). In practice, this kind of plot might prove to be of limited value because visualizing a 3-D image on a 2-D surface is difficult unless it can be rotated using an animated sequence of images (e.g., on a video screen).

4.3. Fundamental Limits to Expected Agreement Between Simulated and Observed Fields

Even if all errors could be eliminated from a model and even if observational uncertainties could be reduced to zero, the simulated and observed climates cannot be expected to be identical because internal (unforced) variations of climate (i.e., noise in this context) will never be exactly the same. Although a good model should be able to simulate accurately the frequency of various unforced weather and climate events, the exact phasing of those events cannot be expected to coincide with the observational record (except in cases where a model is initialized from observations and has not yet reached fundamental predictability limits). The noise of these unforced variations prevents exact agreement between simulated and observed climate. In order to estimate how well a perfect model should agree with perfectly accurate observations, one can again consider differences in individual members of the ensemble of simulations generated by a single model, this time comparing the individual members to each other. Any differ-
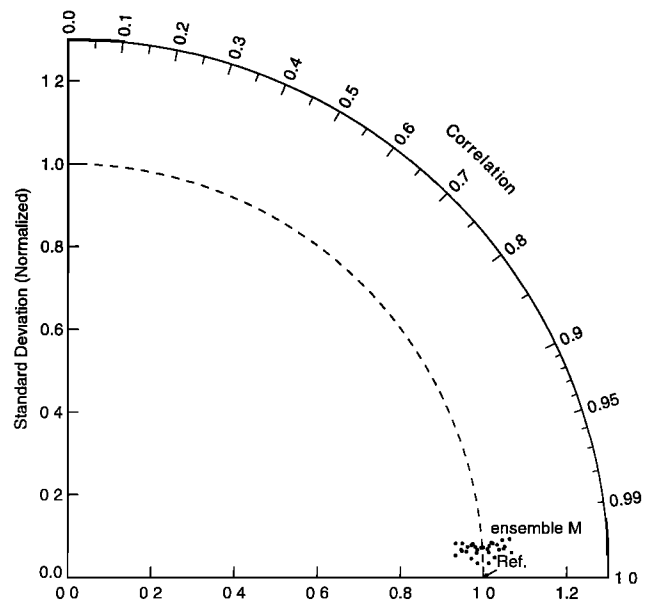

Figure 8. Normalized pattern statistics showing differences within a six-member ensemble of simulations by model M. Thirty points are plotted, two for each pair of ensemble members; one with the first realization taken as the reference and the other with the second realization taken as the reference. The correlation for each pair is not, of course, dependent on which realization is chosen as the reference, but the ratio of their standard deviations is dependent, so the points scatter symmetrically about the arc drawn at unit distance from the origin. Only 15 points are truly independent.

ences in the individual ensemble members must arise from the unforced variations that also fundamentally limit potential agreement between model-simulated and observed climate.

As an illustration of this point, the normalized statistics for rainfall over India have been computed between pairs of simulations comprising model M's six-member ensemble. Each realization of the climatic state is compared to the others, yielding 15 unique pairs. The statistics obtained by considering one realization of each pair as the reference field and the other as the test field are plotted as dots in Figure 8. The high correlation between pairs of realizations indicates that according to this model (run under AMIP experimental conditions) the monthly mean climatology of rainfall over India (calculated from 10 simulated years of data) is largely determined by the imposed boundary conditions (i.e., insolation pattern, sea surface temperatures, etc.) and that noise resulting from internal variations is relatively small. If the unforced variability, which gives rise to the scatter of points in Figure 8, is realistically represented by model M, then even the most skillful of AMIP models can potentially be improved by a substantial amount before reaching the fundamental limits to agreement imposed by essentially unpredictable internal variability. A related conclusion is that since the correlations between modeled and observed patterns shown in Figure 3 are smaller than any of the intraensemble correlations shown in Figure 8, it is likely that the apparent differences between model results and observations are, in fact, statistically significant and could not be accounted for by sampling differences.

Note that in Figure 8 the spread of ensemble points in the radial direction indicates the degree to which unforced vari-
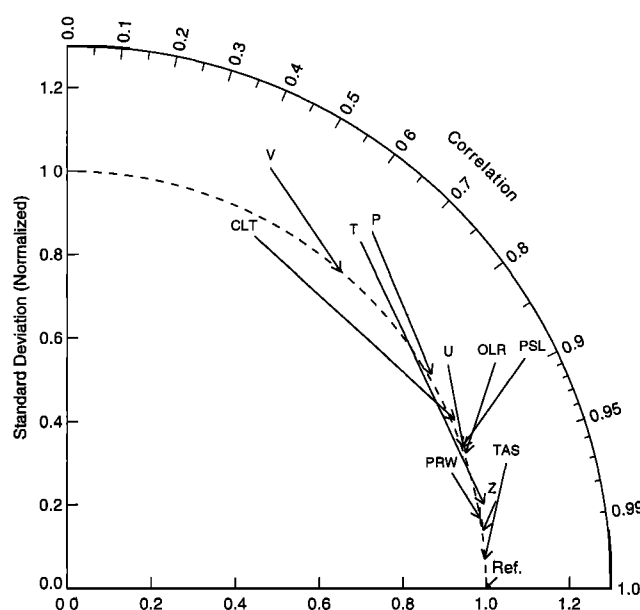
Figure 9. Pattern statistics for one of the AMIP models (indicated by the tail of each arrow) and an estimate of the maximum, potentially attainable agreement with observations, given unforced internal weather and climate variations, as inferred from an ensemble of simulations by model M (indicated by the head of each arrow). The fields shown are described in Figure 5. In contrast to Figure 5, which shows statistics computed from the annual cycle climatology (in which 12 climatological monthly mean samples were used in computing the statistics at each grid cell), here the full space-time statistics are plotted (i.e., 120 time samples, accounting for year-to-year variability, are used in computing the statistics).

ability affects the pattern amplitude, whereas the spread in azimuthal angle is related to its effect on the phase. Also note that in the case of the amplitude of annual cycle of India rainfall, observational uncertainty limits the expected agreement between simulated and observed patterns even more than unforced variability. Finally, note that in AMIP-like experiments the differences in climatological statistics computed from different members of an ensemble will decrease as the number of years simulated increases. Thus, compared to the 10-year AMIP simulation results shown in Figure 8, one should expect that in a similar 20-year AMIP simulation, the points would cluster closer together and move toward the abscissa.

Figure 9 provides another example in which the diagram is used to indicate how far a model is from potentially realizable statistical agreement with observations. For each field the arrows originate at the point comparing an observed field to the corresponding field simulated by a particular AMIP model. The arrows terminate at points indicating the maximum agreement attainable, given internal variability in the system. The model shown in Figure 9 is one of the better AMIP models, and the estimates of the fundamental limits to agreement are obtained from model M's ensemble of AMIP simulations, as described above (with the arrowhead located at the center of the cluster of points). The longer the arrow, the greater the potential for model improvement. For some fields (e.g., cloud fraction and precipitation) the model is far from the fundamental limits, but for others (e.g., geopotential height), there is very little room for improvement in the statistics given here.

In contrast to the climatological mean pattern statistics given

in Figure 5 (computed from the climatological annual cycle data), Figure 9 shows statistics calculated from the 120 individual monthly mean fields available from the 10-year AMIP simulations (thereby including interannual variability). The statistical differences among the individual monthly mean fields are generally larger than the differences between climatological fields because a larger fraction of the total variance is ascribable to unforced, internal variability. Thus in Figure 9 the arrowheads lie farther from the reference point than the corresponding statistics calculated from climatological annual cycle data. Note also that according to Figure 9, there are apparently large differences in the potential for agreement between simulated and observed data, depending on the field analyzed. These differences are determined by the relative contributions of forced and unforced variability to the total pattern of variation of each field.

Boer and Lambert [2001] have suggested an alternative way to factor out the weather and climate noise which limit agreement between simulated and observed fields. They estimate the limits to agreement between simulated and observed patterns of variability that can be expected in the face of unforced natural variability and then rotate each point in the diagram clockwise about the origin such that the distance to the reference point (located at unit distance along the abscissa) is now proportional to the error in the pattern that remains after removing the component that is expected to be uncorrelated with the observed. This modification has the virtue that for all fields, independent of the differing influence of internal variability, the "goal" is the same: to reach the reference point along the x axis. There are, however, disadvantages in rotating the points. The correlation coefficient between the modeled and observed field no longer appears on the diagram but instead is replaced by an "effective" correlation coefficient, which is defined as a weighted difference between two true correlation coefficients. Because the effective correlation coefficient is a derived quantity, interpretation is more difficult. For example, if the interannual variability (i.e., interannual anomalies) simulated by an unforced coupled atmosphere/ocean GCM were compared to observations, the true correlation would be near zero (even for a realistic model), whereas the effective correlation would be near 1, even for a poorly performing model. This difference in true versus effective correlation could cause confusion. One could also argue that explicitly indicating the limits to potential agreement between simulated and observed fields, as in Figure 8, provides useful information that would be hidden by *Boer and Lambert*'s [2001] diagram.

5. Evaluating Model Skill

In the case of mean sea level pressure in Figure 5 the correlation decreased (indicating lower pattern similarity) but the RMS error was reduced (indicating closer agreement with observations). Should one conclude that the model skill has improved or not? A relatively skillful model should be able to accurately simulate both the amplitude and pattern of variability. Which of these factors is more important depends on the application and to a certain extent must be decided subjectively. Thus it is not possible to define a single skill score that would be universally considered most appropriate. Consequently, several different skill scores have been proposed [e.g., *Murphy*, 1988; *Murphy and Epstein*, 1989; *Williamson*, 1995; *Watterson*, 1996; *Watterson and Dix*, 1999; *Potts et al.*, 1996].

Nevertheless, it is not difficult to define attributes that are desirable in a skill score. For any given variance the score should increase monotonically with increasing correlation, and for any given correlation the score should increase as the modeled variance approaches the observed variance. Traditionally, skill scores have been defined to vary from zero (least skillful) to one (most skillful). Note that in the case of relatively low correlation the inverse of the RMS error does not satisfy the criterion that skill should increase as the simulated variance approaches the observed. Thus a reduction in the RMS error may not necessarily be judged an improvement in skill.

One of the least complicated scores that fulfills the above requirements is defined as

$$S = \frac{4(1 + R)}{(\hat{\sigma}_f + 1/\hat{\sigma}_f)^2 (1 + R_0)},$$ (4)

where R_0 is the maximum correlation attainable (according to the fundamental limits discussed in section 4.3 and as indicated, for example, by the position of the arrowheads in Figure 9). As the model variance approaches the observed variance (i.e., as $\hat{\sigma}_f \to 1$) and as $R \to R_0$, the skill approaches unity. Under this definition, skill decreases toward zero as the correlation becomes more and more negative or as the model variance approaches either zero or infinity. For fixed variance the skill increases linearly with correlation. Note also that for small model variance, skill is proportional to the variance, and for large variance, skill is inversely proportional to the variance.

The above skill score can be applied to the India rainfall statistics shown in Figure 3, which are plotted again in Figure 10 along with contours of constant skill. The skill score was defined with R_0 set equal to the mean of the 30 intraensemble correlation values shown in Figure 8 (i.e., $R_0 = 0.9976$). In addition to the properties guaranteed by the formulation, skill
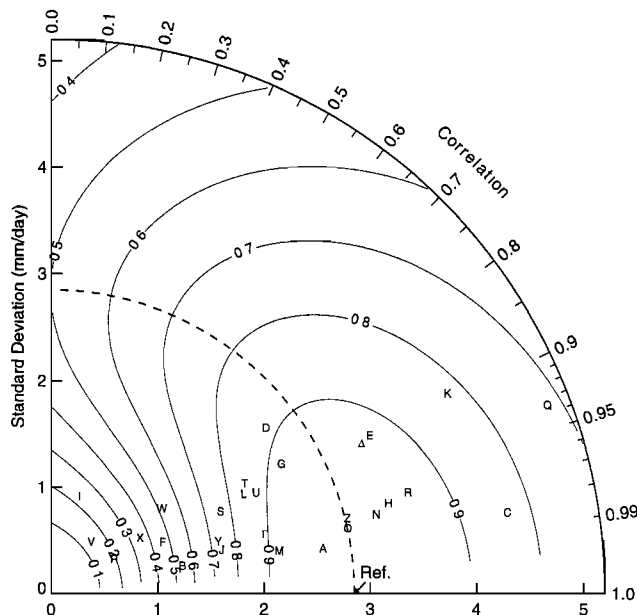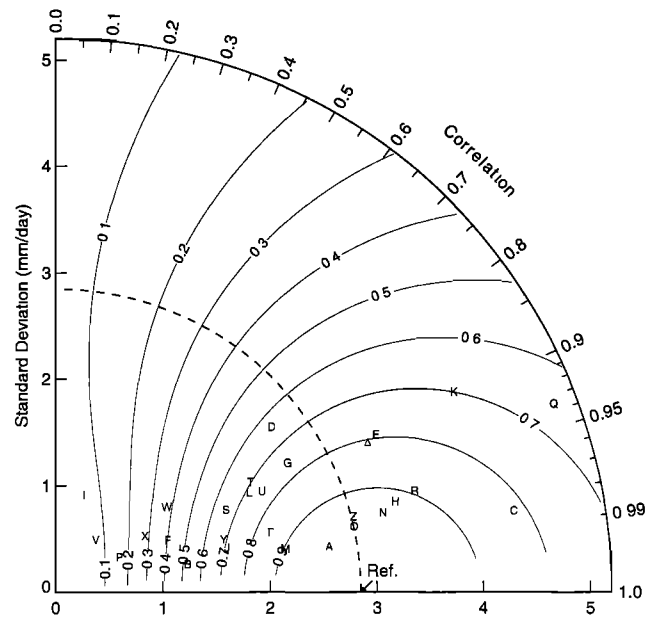

Figure 11. As in Figure 10, but for an alternative measure of skill defined by (5).

is seen to decrease generally with increasing RMS error, but at low correlation, models with too little variability are penalized. If in a particular application such a penalty were considered too stiff, a different skill score could be devised that would downweight its importance.

Under the above definition the skill depends on R_0, which is the maximum potentially realizable correlation, given the noise associated with unforced variability. Estimates of R_0 are undoubtedly model-dependent, and for that reason, the value of R_0 should always be recorded whenever a skill score is reported.

According to the skill score defined by (4), model E is slightly more skillful than model M in spite of its poorer correlation. To increase the penalty imposed for low correlation, (4) could be slightly modified as follows:

$$S = \frac{4(1 + R)^4}{(\hat{\sigma}_f + 1/\hat{\sigma}_f)^2 (1 + R_0)^4}.$$ (5)

Once again the India rainfall statistics can be plotted, this time drawing the skill score isolines defined by (5). Figure 11 shows that according to this skill score, model E would now be judged less skillful than model M. This illustrates that it is not difficult to define skill scores that preferentially reward model-simulated patterns that are highly correlated with observations or, alternatively, place more emphasis on correct simulation of the pattern variance.

6. Summary and Further Applications

The diagram proposed here provides a way of plotting on a 2-D graph three statistics that indicate how closely a pattern matches observations. These statistics make it easy to determine how much of the overall RMS difference in patterns is attributable to a difference in variance and how much is due to poor pattern correlation. As shown in the examples, the diagram can be used in a variety of ways. The first example involved comparison of the simulated and observed climato-

Figure 10. Isolines of one suggested measure of skill, as defined by (4), drawn on a diagram that indicates pattern statistics for the climatological annual cycle of precipitation over India simulated by 28 models.

logical annual cycle of precipitation over India. The new diagram made it easy to distinguish among 28 models and to determine which models were in relatively good agreement with observations. In other examples, the compared fields were functions of both space and time, in which case, direct visual comparison of the full simulated and observed fields would be exceedingly difficult. In this case, statistical measures of the correspondence between modeled and observed fields offered a practical way of assessing and summarizing model skill.

The diagram described here is beginning to see use in some recent studies [e.g., *Räisänen*, 1997; *Gates et al.*, 1999; *Lambert and Boer*, 2001], and one can easily think of a number of other applications where it might be especially helpful in summarizing an analysis. For example, it is often quite useful to resolve some complex pattern into components and then to evaluate how well each component is simulated. Commonly, fields are resolved into a zonal mean component plus a deviation from the zonal mean. Similarly, the climatological annual cycle of a pattern is often considered separately from the annual mean pattern or from "anomaly" fields defined as deviations from the climatological annual cycle. It can be useful to summarize how accurately each individual component is simulated by a model, and this can be done on a single plot. Similarly, different scales of variability can be extracted from a pattern (through filtering or spectral decomposition), and the diagram can show how model skill depends on scale.

Although the diagram has been designed to convey information about centered pattern differences, it is also possible to indicate differences in overall means (i.e., the bias defined in section 2). This can be done on the diagram by attaching to each plotted point a line segment drawn at a right angle to the straight line defined by the point and the reference point. If the length of the attached line segment is equal to the bias, then the distance from the reference point to the end of the line segment will be equal to the total (uncentered) RMS error (i.e., bias error plus pattern RMS error), according to (3).

An ensemble of simulations by a single model can be used both in the assessment of statistical significance of apparent differences and also to estimate the degree to which internal weather and climate variations limit potential agreement between model simulations and observations. In the case of multiannual climatological fields these fundamental limits to agreement generally decrease with the number of years included in the climatology (under an assumption of stationarity). However, in the case of statistics computed from data that have not been averaged to suppress the influence of unforced internal variability (e.g., a monthly mean time series that includes year-to-year variability) the differences between model-simulated and observed fields cannot be expected to approach zero, even if the model is perfect and the observations are error free. These fundamental limits to agreement between models and observations are different for different fields and will generally vary with the time and space scales considered. One consequence of this fact is that a field that is rather poorly simulated may have relatively little potential for improvement compared to another field that is better simulated.

Two different skill scores have also been proposed here, but these were offered as illustrative examples and will, it is hoped, spur further work in this area. It is clear that no single measure is sufficient to quantify what is perceived as model skill, even for a single variable, but some of the criteria that should be

considered have been discussed. The geometric relationship between the RMS difference, the correlation coefficient, and the ratio of variances between two patterns, which underlies the diagram proposed here, may provide some guidance in devising skill scores that appropriately penalize for discrepancies in variance and discrepancies in pattern similarity.

References

Boer, G. J., and S. J. Lambert, Second order space-time climate difference statistics, *Clim. Dyn.*, *17*, 213–218, 2001.

Gates, W., et al., An overview of the results of the Atmospheric Model Intercomparison Project (AMIPI), *Bull. Am. Meteorol. Soc.*, *80*, 29–55, 1999.

Gibson, J. K., P. Kållberg, S. Uppala, A. Hernandez, A. Nomura, and E. Serrano, ERA description, *ECMWF Re-anal. Proj. Rep. Ser. 1*, 66 pp., Eur. Cent. for Medium-Range Weather Forecasts, Reading, England, 1997.

Harrison, E. P., P. Minnis, B. R. Barkstrom, V. Ramanathan, R. D. Cess, and G. G. Gibson, Seasonal variation of cloud radiative forcing derived from the Earth Radiation Budget Experiment, *J. Geophys. Res.*, *95*, 18,687–18,703, 1990.

Jones, P. D., M. New, D. E. Parker, S. Martin, and I. G. Rigor, Surface air temperature and its changes over the past 150 years, *Rev. Geophys.*, *37*, 173–199, 1999.

Lambert, S. J., and G. J. Boer, CMIP1 evaluation and intercomparison of coupled climate models, *Clim. Dyn.*, *17*, 83–106, 2001.

Murphy, A. H., Skill scores based on the mean square error and their relationship to the correlation coefficient, *Mon. Weather Rev.*, *116*, 2417–2424, 1988.

Murphy, A. H., and E. S. Epstein, Skill scores and correlation coefficients in model verification, *Mon. Weather Rev.*, *117*, 572–581, 1989.

Parthasarathy, B., A. A. Munot, and D. R. Kothawale, All-India monthly and seasonal rainfall series: 1871–1993, *Theor. Appl. Climatol.*, *49*, 217–224, 1994.

Potts, J. M., C. K. Folland, I. T. Jolliffe, and D. Sexton, Revised "LEPS" scores for assessing climate model simulations and long-range forecasts, *J. Clim.*, *9*, 34–53, 1996.

Räisänen, J., Objective comparison of patterns of CO_2 induced climate change in coupled GCM experiments, *Clim. Dyn.*, *13*, 197–211, 1997.

Rossow, W. B., and A. Schiffer, ISCCP cloud data products, *Bull. Am. Meteorol. Soc.*, *72*, 2–20, 1991.

Watterson, I. G., Non-dimensional measures of climate model performance, *Int. J. Climatol.*, *16*, 379–391, 1996.

Watterson, I. G., and M. R. Dix, A comparison of present and doubled CO_2 climates and feedbacks simulated by three general circulation models, *J. Geophys. Res.*, *104*, 1943–1956, 1999.

Wilks, D. S., Resampling hypothesis tests for autocorrelated fields, *J. Clim.*, *10*, 65–82, 1997.

Williamson, D. L., Skill scores from the AMIP simulations, in *Proceedings of the First International AMIP Scientific Conference*, edited by W. L. Gates, *WMO TD-732*, pp. 253–258, World Meteorolog. Organ., Geneva, Switzerland, 1995.

Xie, P., and P. Arkin, Global precipitation: A 17-year monthly analysis based on gauge observations, satellite estimates, and numerical model outputs, *Bull. Am. Meteorol. Soc.*, *78*, 2539–2558, 1997.

K. E. Taylor, Program for Climate Model Diagnosis and Intercomparison, Lawrence Livermore National Laboratory, MS L-264, P.O. Box 808, Livermore, CA 94550. (taylor13@llnl.gov)